Neuropharmacology 95 (2015) 468–476

Contents lists available at ScienceDirect

Neuropharmacology

journal homepage: www.elsevier.com/locate/neuropharm

Dopaminergic and cholinergic modulation of striatal tyrosine hydroxylase interneurons

Osvaldo Ibáñez-Sandoval [1], Harry S. Xenias [2], James M. Tepper[*], Tibor Koós[**]

Center for Molecular and Behavioral Neuroscience, Rutgers The State University of New Jersey, 197 University Avenue, Newark, NJ 07102, USA

ARTICLE INFO

Article history:
Received 22 August 2013
Received in revised form
17 March 2015
Accepted 31 March 2015
Available online 20 April 2015

Keywords:
Neostriatum
GABAergic
TH
Dopamine
ACh
Plateau potential

ABSTRACT

The recent electrophysiological characterization of TH-expressing GABAergic interneurons (THINs) in the neostriatum revealed an unexpected degree of diversity of interneurons in this brain area (Ibáñez-Sandoval et al., 2010, Unal et al., 2011, 2015). Despite being relatively few in number, THINs may play a significant role in transmitting and distributing extra- and intrastriatal neuromodulatory signals in the striatal circuitry. Here we investigated the dopaminergic and cholinergic regulation of THINs *in vitro*. We found that the dominant effect of dopamine was a dramatic enhancement of the ability of THINs to generate long-lasting depolarizing plateau potentials (PPs). Interestingly, the same effect could also be elicited by amphetamine-induced release of endogenous dopamine suggesting that THINs may exhibit similar responses to changes in extracellular dopamine concentration *in vivo*. The enhancement of PPs in THINs is perhaps the most pronounced effect of dopamine on the intrinsic excitability of neostriatal neurons described to date. Further, we demonstrate that all subtypes of THINSs tested also express nicotinic cholinergic receptors. All THINs responded, albeit differentially, with depolarization, PPs and spiking to brief application of nicotinic agonists. Powerful modulation of the nonlinear integrative properties of THINs by dopamine and the direct depolarization of these neurons by acetylcholine may play important roles in mediating the effects of these neuromodulators in the neostriatum with potentially important implications for understanding the mechanisms of neuropsychiatric disorders affecting the basal ganglia.

1. Introduction

Until recently, the neostriatum has been thought to contain only a few types of GABAergic interneurons in comparison to the large diversity of GABAergic cell types in the neocortex or the hippocampus (Freund and Buzsáki, 1996; Tepper et al., 2010; DeFelipe et al., 2013). This picture changed significantly with the introduction of transgenic reporter mouse lines that revealed the existence of 5 new electrophysiologically distinct cell types, more than doubling the number of interneuron classes recognized in this brain area (Ibáñez-Sandoval et al., 2010; Ibáñez-Sandoval et al., 2011; Unal et al., 2011). In addition to a neuropeptide Y (NPY) expressing neuron described in a NPY-GFP line (Ibáñez-Sandoval et al., 2011), the newly discovered interneurons include 4 additional types of GABAergic neurons that were termed TH-interneurons (THINs) reflecting their initial identification in a TH-EGFP strain (Ibáñez-Sandoval et al., 2010; Unal et al., 2011). The function of THINs remains unclear. Their small population size and connectivity place some important constraints on the possible function of these neurons. On particularly interesting possibility is that these neurons may distribute intra- and extrastriatal neuromodulatory signals to projection neurons.

In the neostriatum, dopamine (DA) and acetylcholine (ACh) are 2 major neuromodulators that exert pronounced effects on most functions of the basal ganglia. Here we investigated how these neuromodulators or control the intrinsic electrophysiological properties of THINs. Since preliminary experiments indicated that the most salient effect of these modulators was the triggering and enhancement of a semi-stable depolarizing state we characterized in more detail this important dynamic feature of THINs.

* Corresponding author. Tel.: +1 973 353 3618; fax: +1 973 353 1588.
** Corresponding author. Tel.: +1 973 353 1080x3638; fax: +1 973 353 1588.
E-mail addresses: jtepper@andromeda.rutgers.edu (J.M. Tepper), tibkoos@yahoo.com (T. Koós).
[1] Present address: Departamento de Fisiología, Facultad de Medicina, Universidad Autónoma de San Luis Potosí, Av., Venustiano Carranza, San Luis Potosí, Mexico.
[2] Present address: Department of Physiology, Feinberg School of Medicine, Northwestern University, Chicago, IL, USA.

http://dx.doi.org/10.1016/j.neuropharm.2015.03.036
0028-3908/

2. Materials and methods

2.1. Subjects

We used transgenic mice Tg (Th-EGFP) DJ76Gsat/Mmmc (GENSAT; Gong et al., 2003), obtained from the Mutant Mouse Regional Resource Center at UCLA and bred in our colony at Rutgers for all experiments. Hemizygous progeny were mated to wild type FVB or Swiss Webster mice each generation thereafter. All offspring were genotyped from tail samples and only those expressing the EGFP transgene were used in these experiments. Henceforth these mice are referred to as EGFP-TH mice.

All procedures were performed with the approval of the Rutgers University Institutional Animal Care and Use Committee and in accordance with the NIH *Guide to the Care and Use of Laboratory Animals* and all efforts were made to minimize the number of mice used and any possible discomfort.

2.2. Preparation of brain slices

Experiments were performed on brain slices obtained from adult EGFP-TH mice older than one month of age. Mice were deeply anesthetized with 150 mg/kg ketamine and 30 mg/kg xylazine i.p. and transcardially perfused with ice-cold, modified Ringer's solution containing (in mM) 248 sucrose, 2.5 KCl, 7 MgCl2, 23 $NaHCO_3$, 1.2 NaH_2PO_4, 7 glucose, 1 ascorbate, 3 pyruvate, and bubbled with 95% O_2 and 5% CO_2 (pH 7.3). The brain was quickly removed into a beaker containing ice-cold oxygenated Ringer's and trimmed to a block containing the striatum. Coronal or para-horizontal sections (250–300 μm) were cut in the same medium using a Vibratome 3000 and immediately transferred to normal Ringer's solution containing (in mM) 124 NaCl, 2.5 KCl, 1.2 NaH_2PO_4, 26 $NaHCO_3$, 1.3 $MgCl_2$, 2 $CaCl_2$, 10 glucose, 1 ascorbate, 3 pyruvate, and 0.4 myo-inositol that was heated to 34 °C and continuously bubbled with 95% O_2 and 5% CO_2 (pH 7.3) for 1 h prior to recording and then maintained at room temperature until use. In some experiments, we substituted in an equimolar manner: choline Cl for NaCl, choline bicarbonate for $NaHCO_3$ and sucrose for $CaCl_2$. Slices were transferred to the recording chamber and submerged in continuously flowing oxygenated buffer (2–4 ml/min) which was heated with an inline heater (Warner Instruments) to approximately 33 °C.

2.3. Fluorescence and DIC imaging and recording

Slices were initially visualized under epifluorescence illumination with a high sensitivity digital frame transfer camera (Cooke SensiCam) mounted on an Olympus BX50-WI epifluorescence microscope and a 40× long working distance water immersion lens. Once an EGFP-TH neuron was identified, visualization was switched to infrared differential interference contrast (IR-DIC) microscopy for the actual patching of the neuron, usually performed under current clamp.

Micropipettes for whole cell recording were constructed from 1.2 mm o.d. and 0.94 mm i.d. borosilicate pipettes (Harvard apparatus) on a Narishige PP-83 vertical puller. The standard internal solution for whole cell current clamp recording was (in mM): 130 K gluconate, 10 NaCl, 2 $MgCl_2$, 10 HEPES, 3 Na_2ATP, 0.3 GTP, 1 EGTA plus 0.1–0.3% biocytin (pH 7.3–7.4). These pipettes typically exhibited a DC impedance of 4–6 MΩ measured in the recording chamber.

Current clamp recordings were made with a Neurodata IR-283 current clamp amplifier and voltage and/or current clamp recordings were made with a Multiclamp 700B amplifier (Molecular Devices, Sunnyvale, CA) whose output was filtered online with a second order Bessel filter at 1 kHz and digitized at 20-40 KHz with either a CED Micro 1401 Mk II and a PC running Signal v. 4 (Cambridge Electronic Design, Cambridge UK) or an ITC-16 and a Mac running Axograph. Acquired data was stored on a PC or Mac for offline analysis.

At the completion of the experiments slices containing biocytin-injected neurons were fixed by immersion in 4% paraformaldehyde-0.5% glutaraldehyde for 30 min at room temperature or microwaved to 60 °C for 12 s and stored overnight at 4 °C.

2.4. Pharmacology

Drugs were applied in the perfusion medium or locally via a micropipette using a Picospritzer (General Valve, Fairfield, NJ), at 20 psi/30–100 ms, at 0.1 Hz. Nimodipine, flufenamic acid, SCH-23390 hydrochloride, SKF-38393 hydrochloride, dopamine, choline bicarbonate and amphetamine were purchased from Sigma–Aldrich and tetrodotoxin (TTX), carbamylcholine chloride (carbachol), mecamylamine hydrochloride (MEC), Dihydro-β-erythroidine hydrobromide (DHβE) and methyllycaconitine citrate (MLA) were purchased from Tocris. Nimodipine and flufenamic acid were dissolved in dimethyl sulfoxide. All other drugs were dissolved freshly in Ringer's solution.

2.5. Extracellular stimulation

Stimulating electrodes consisted of concentric bipolar electrodes of 25 μm at the tip, and 1 kΩ DC resistance were used (FHC, Bowdoinham, ME). Electrodes were placed onto the surface of the slice within 200–500 μm of the recorded cells. Stimuli consisted of single square wave pulses (typically 0.01–1 mA, 200 μs duration at 0.1–0.5 Hz) and was generated by a Winston A-65 timer and SC-100 constant current stimulus isolation unit (eg., Lee and Tepper, 2007; Ibánez-Sandoval et al., 2010).

2.6. Biocytin histochemistry

Slices containing biocytin-filled neurons were transferred into 4% paraformaldehyde overnight. In some cases, the thick sections were resectioned on a Vibratome at 100 μm. Sections were washed for 3 × 10 min in 0.1 M phosphate buffer (PB) followed by 10% methanol and 3% H_2O_2 for 15 min, and incubated with avidin-biotin-peroxidase complex (Vector Laboratories; 1:200) and 0.1% Triton X-100 overnight at 4 °C. After washing 6 × 10 min in 0.1 M PB the sections were reacted with 3,-3′-diaminobenzidine (DAB; 0.025%) and H_2O_2 (0.0008%) in PB. In some cases nickel intensification (Adams, 1981) was used (2.5 mM nickel ammonium sulfate and 7 mM ammonium chloride in the DAB and H_2O_2 incubation). The sections were then postfixed in osmium tetroxide (0.1% in PB) for 30 min, dehydrated through a graded series of ethanol, followed by propylene oxide, and infiltrated overnight with a mixture of propylene oxide and epoxy resin (Durcupan; Fluka Chemie, Buchs, Switzerland). The sections were then transferred to fresh resin mixture for several hours and flat embedded between glass slides and coverslips and polymerized at 60 °C for 24 h.

2.7. Statistical analysis

Most numerical values are reported as the mean ± SEM. Data were analyzed by using ANOVA with Prism (GraphPad Software), followed with Tukey's post hoc tests to multiple comparisons means. Differences were considered to be significant at $p < 0.05$.

3. Results

3.1. Electrophysiological and anatomical properties of striatal TH interneurons

Ex vivo whole-cell recordings were obtained in current clamp mode from fluorescent neurons in the striatum of adult EGFP-TH mice. In agreement with previously reported data (Ibáñez-Sandoval et al., 2010), several distinct subtypes of THINs could be characterized on the basis of their intrinsic electrophysiological properties (input resistance R_{in}), resting membrane potential (RMP), action potential duration at half-amplitude ($AP_{50\%}$), their ability or inability to maintain firing throughout modest depolarizing current injections and the presence of a low-threshold spike (LTS). These were: Type I (R_{in} = 554 ± 48 MΩ, RMP = −63 ± 2 mV and $AP_{50\%}$ = 1 ± 0.08 ms; n = 45/68 [66%]), Type II (R_{in} = 379 ± 79 MΩ, RMP = −75 ± 2 mV and $AP_{50\%}$ = 0.45 + 0.03 ms; n = 8/68 [12%]), and Type IV (R_{in} = 486 ± 67 MΩ, RMP = −75 ± 1 mV, $AP_{50\%}$ = 0.61 + 0.06 ms and LTS; n = 15/68 [22%]). Type III striatal THINs that made up only about 5% of the total population in our original study (Ibáñez-Sandoval et al., 2010) were not encountered in the present study, while the remaining subtypes were present in roughly the same proportions as reported previously. Representative examples of responses to current injection and the resulting current–voltage curves for Type I, II and IV THINs are shown in Fig. 1.

Striatal THINs frequently (46%, 21/45 of Type I, and 25%, 2/8 of Type II) exhibited an intrinsic PP in response to strong depolarizing current pulses delivered at rest as previously described (Ibáñez-Sandoval et al., 2010). PPs ranged in duration from 15 ms to over 5 s. A typical example of a PP from a Type I striatal THIN is shown in Fig. 1.

During whole cell recordings, all neurons were filled with biocytin for subsequent anatomical study. Eleven neurons were chosen for further anatomical analysis. These neurons exhibited morphologies consistent with our previous reports (Ibáñez-Sandoval et al., 2010; Tepper et al., 2010). Striatal THIN somata were medium sized (14.5 ± 1 μm × 10 ± 0.5 μm) and emitted from 2 to 5 thick primary dendrites that branched modestly, forming a simple dendritic arborization rarely exceeding 300 microns in diameter. The dendrites of many Type I neurons were sparsely invested with spine-like spines processes. The most characteristic feature of the THINs was their axon arborization. The axon

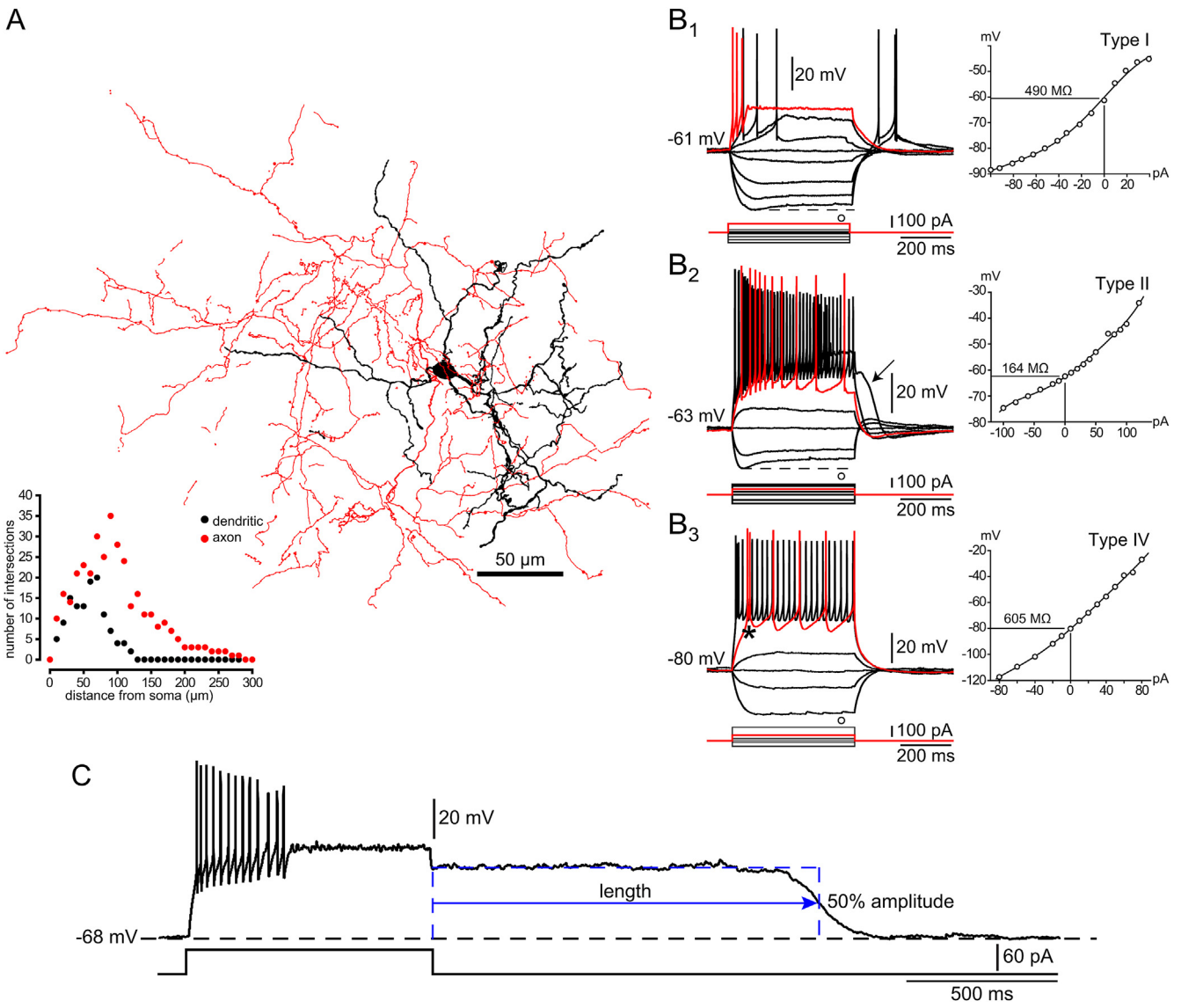

Fig. 1. Anatomical and electrophysiological characteristics of striatal THINs recorded in adult EGFP-TH mice A. Drawing tube reconstruction of a representative striatal Type I THIN filled with biocytin after whole-cell recording. Dendrites are drawn in black and the axon in red. Inset: Sholl plot data. B. Examples of voltage responses to hyperpolarizing and depolarizing current injection pulses illustrate the typical passive electrophysiological properties that distinguish Type I (B1), Type II (B2) and Type IV (B3) striatal THINs. C. Type I THINs frequently exhibit (~41%) an intrinsic plateau potential (PP) following depolarization from rest that long outlasts the stimulus, illustrated here to show methods used to quantify PPs. (For interpretation of the references to color in this figure legend, the reader is referred to the web version of this article.)

originated from the soma or proximally from a primary dendrite, and branched extensively creating a dense arborization overlapping and extending beyond the dendritic field. Axons exhibited very prominent, evenly spaced varicosities, presumably boutons en passant, throughout the axonal field. A typical example is shown in Fig. 1. The other three subtypes of THINS were aspiny, exhibited moderately varicose dendrites, and were indistinguishable anatomically from one another.

3.2. Ionic characterization of plateau potential of striatal TH interneurons

The ionic basis of the intrinsic PP was analyzed in current clamp recordings from a subset of striatal THINs exhibiting robust PPs. In this subset, the mean PP duration was 1258 ± 344 ms (range, 495 ms–2626 ms, n = 6). PPs were characterized by a strong and sustained depolarization of the membrane potential, upon which truncated spikes sometimes rode. Substitution of Na^+ by choline (Fig. 2A1, red traces; Na^+-free), abolished the spikes and significantly reduced the PP duration to 405 ± 122 ms (range: 59–869 ms, control vs. Na^+-free, $p < 0.05$, n = 6). Subsequent substitution of Ca^{2+} by sucrose (Fig. 2A1, gray traces; Ca^{2+}-free), eliminated the PP entirely, reducing the duration to 5 ± 3 ms (range, 0–17 ms, control vs. Ca^{2+}-free, $p < 0.001$, n = 6). These results demonstrate that a sodium conductance was responsible for the generation of the spikes seen riding on the PP, which also contributes to the PP itself, and that Ca^{2+} entry was essential for the activation of the PP. Washing in normal buffer caused a partial recovery of both spikes and the PP at a duration of 795 ± 199 ms (range, 323–1323 ms, control vs. recovered $p > 0.05$, n = 6), as shown in Fig. 2A1. Addition of either nimodipine (10 μM) or flufenamic acid (100 μM) completely abolished the PP (Fig. 2A1, blue traces) (range, 0–28 ms, control vs. NIM/FFA $p < 0.001$, n = 6). Taken together, these results confirm our previous results that the intrinsic PPs are due to a Na^+

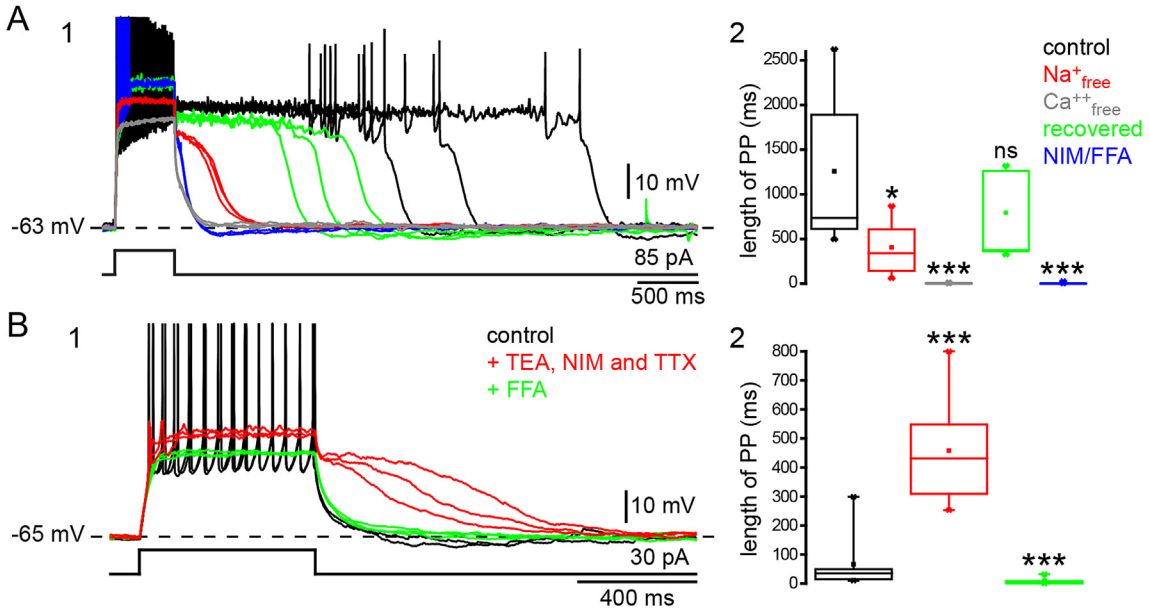

Fig. 2. Ionic mechanisms underlying the PP. A1. PPs evoked under control conditions (black traces) were reduced by over 75% when Na^+ was replaced by choline (red traces), illustrated here in a Type I THIN. Replacement of Ca^{2+} by sucrose completely eliminated the PP (gray traces). Partial recovery of the PP when buffer returned to control conditions (green traces). Either nimodipine (NIM; 10 μM), an L-type calcium channels blocker, or flufenamic acid (FLU; 100 μM), a calcium-activated nonselective cation conductance blocker, completely blocked the PP (blue traces, data for NIM and FFA combined). A2. Summary box plots of six experiments. B1. Example of a striatal Type IV THIN that did not exhibit intrinsic PPs (black traces). In these cases, addition of TEA (20 mM) consistently unmasked PP (red traces), even in present of NIM (10 μM) and TTX (1 μM). TEA evoked PPs were also completely eliminated by FFA (100 μM) (green traces). B2. Summary box plots of seven experiments. Box borders represent 25th and 75th percentiles. Whiskers represent data minima and maxima. Line represents median. Point represents mean. * indicates $p < 0.05$ and *** indicates $p < 0.001$ with respect to control. ns indicates $p > 0.05$ with respect to control. Action potentials are truncated to illustrate subthreshold events. (For interpretation of the references to color in this figure legend, the reader is referred to the web version of this article.)

and L-type Ca^{2+} dependent calcium-activated nonselective cation current, I_{CAN}, as suggested previously (Ibáñez-Sandoval et al., 2010). I_{CAN} is likely related to a melastatin-related transient receptor potential cation channel (TRPM), most likely TRPM2 (Fleig and Penner, 2004; Hill et al., 2004; Lee and Tepper, 2007). Further, the strong inhibitory effect of nimodipine applied alone demonstrates that under these conditions L-type channels supply the intracellular Ca^{2+} required for I_{CAN} activation (Fleig and Penner, 2004; Hill et al., 2004; Lee and Tepper, 2007).

In striatal THINs that did not exhibit intrinsic PPs, TEA (20 mM) was capable of inducing their appearance, as illustrated in Fig. 2B. In striatal THINs that exhibited short duration intrinsic PPs, 66 ± 34 ms (range, 10–299 ms, n = 8), TEA significantly prolonged the PP to 429 ± 65 ms (range, 227–800 ms, control vs. TEA, NIM and TTX $p < 0.001$, n = 8), even in the presence of nimodipine (10 μM) and TTX (1 μM). These results suggest that most or all striatal THINs are capable of generating a PP, but that under most conditions, it is partially or completely masked by a constitutively active TEA sensitive potassium conductance, similar to results reported previously for GABAergic neurons from substantia nigra pars reticulata (Lee and Tepper, 2007).

TEA promotes calcium influx into the cell by a different mechanism than that which is involved in control conditions. TEA-induced PPs are sustained in the presence of L-type Ca^{2+} channel blockade and TTX, but are abolished by flufenamic acid 10 ± 4 ms, (range, 0–32 ms, n = 8) as shown in Fig. 2. Thus, although the PP is normally activated by L-type Ca^{2+} channels under normal conditions, the calcium conductance does not underlie the TEA induced PP itself.

These results indicate that both intrinsic and TEA-induced PPs are generated by the same current, I_{CAN}, similar to plateau potentials exhibited by other neurons in the basal ganglia (Baufreton et al., 2003; Hill et al., 2004; Lee and Tepper, 2007).

3.3. Dopamine modulation of plateau potentials in striatal THINs

Because of the importance of dopaminergic modulation in the basal ganglia and because 6-OHDA lesions reduce or abolish PPs in striatal THINs (Unal et al., 2015), we investigated dopaminergic modulation of the PP in striatal THINs.

In several striatal neurons, both those that exhibited intrinsic PPs and as well as those that did not (mean PP duration 43 ± 12 ms, range, 2–163 ms, n = 12), we explored the effects of amphetamine, which increases the extracellular DA concentration by causing DA release by reverse transport as well as by blocking reuptake (Khoshbouei et al., 2003; Kahlig et al., 2005). In the presence of 50 μM amphetamine (Fig. 3, compare black and blue traces), PPs could be induced or were increased in duration, 354 ± 30 ms (range, 335–577 ms, control vs. amphetamine $p < 0.001$, n = 12). PPs induced or prolonged by amphetamine were, like intrinsic PPs, completely blocked by nimodipine (5 μM) or flufenamic acid (100 μM) (Fig. 3, red traces), 36 ± 6 ms (range, 10–82 ms, amphetamine vs. NIM/FFA $p < 0.001$, n = 12). Thus, PPs can be induced or prolonged by endogenously released DA.

Similarly to amphetamine, 30 μM DA induced or increased the duration of the PP 219 ± 34 ms (range, 69–386 ms; Fig. 3, compare black and green traces) to 710 ± 134 ms (range, 376–1932 ms, control vs. DA $p < 0.001$ n = 11). The effects of exogenous application of DA were also eliminated by nimodipine (5 μM) or flufenamic acid (100 μM), (Fig. 3, red traces), 22 ± 3 ms (range, 9–38 ms, DA vs. NIM/FFA $p < 0.001$, n = 11).

3.4. Dopamine effects on the plateau potential are mediated through D1/D5-like DA receptors

One way that DA could activate or facilitate PPs in striatal THINs is by enhancement of L-type Ca^{2+} currents that promote I_{CAN}

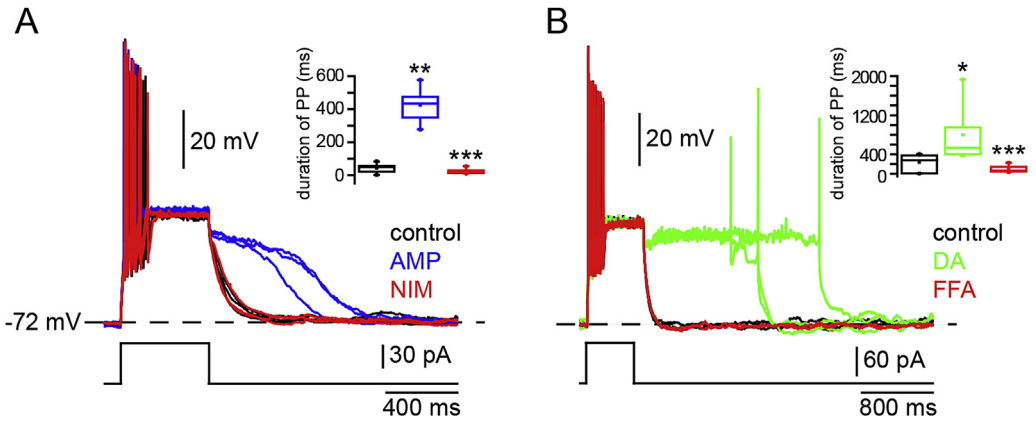

Fig. 3. Dopaminergic modulation of PPs in striatal TH interneurons. A. Type I THIN that does not exhibit an intrinsic PP (black traces). D-Amphetamine (AMP; 50 μM) a PP (blue traces). The amphetamine-induced PP was blocked by nimodipine (NIM; 10 μM) or flufenamic acid (FFA; not shown). B. Another Type I THIN did not exhibit a plateau potential (black traces). Dopamine (DA; 30 μM) induces a long duration PP. Similar to the neuron in A, either FFA or NIM (not shown) completely blocked the plateau potential. (For interpretation of the references to color in this figure legend, the reader is referred to the web version of this article.)

activation. Previous reports showed that D1/D5-like receptor activation enhanced the L-type Ca^{2+} current and discharge of action potentials in striatal SPNs (Hernández-López et al., 1997; Surmeier et al., 1995). Thus, we explored whether DA effects on PPs in striatal THINs were mediated by DA D1/D5 receptors.

DA (30 μm) was bath applied and enhanced PPs as described above from a duration of 275 ± 61 ms (range, 34–475 ms; Fig. 4A1, compare black and red traces) to 2129 ± 862 ms (range, 641–6141 ms, $p < 0.01$, $n = 6$). Subsequent addition of 5 μM SCH-323390, a D1/D5 DA receptor antagonist, reversed the effect of DA as indicated by a significant reduction of the duration of the PP to 532 ± 92 ms (range, 357–965 ms; Fig. 4A2 see green traces, $p > 0.05$, $n = 6$). In some cases the PP was completely eliminated by SCH-323390 (Fig. 4A2). The effect of the antagonist (in the continued presence of DA) recovered partially after washout of SCH-23390 1811 ± 936 ms (range, 593–6429 ms; Fig. 4A2, compare green and blue traces, $p < 0.01$, $n = 6$). In THINs exhibiting DA-evoked PPs, the addition of 10 μM NIM or 100 μM FFA completely blocked the PPs; 51 + 7 ms (range; 36–80 ms; Fig. 4A2, compare blue and magenta traces, ns, $n = 6$). In another group of striatal THINs that did not exhibit PPs in control, long lasting PPs could be induced by the D1/D5-receptor agonist SKF-38393 (5 μM) and these responses could be blocked by co-application of SCH-23390 (5 μM), a selective antagonist for D1/D5-like DA receptors (Fig. 4C1 and C2).

3.5. Striatal TH interneurons express nicotinic cholinergic receptors

Although ACh exerts important effects in the neostriatum through muscarinic receptors, in this study we were primarily interested in the possibility of fast especially nicotinic receptor mediated regulation of THINs. Therefore, we tested the effects of local pressure application of 100 μM carbachol on 3 of the 4 electrophysiologically defined subtypes of THINSs including Type I ($n = 7$), II ($n = 5$) and IV ($n = 8$) neurons. Interestingly, the responses to carbachol were subtype-dependent. Type I THINs, the most common subtype comprising >65% of THINs, responded to brief carbachol application with a strong depolarization that elicited an initial, approximately 100 ms long high frequency burst of rapidly adapting and accommodating spikes, similar to the bursts elicited with strong intracellular depolarizing current injections. The spikes were followed by a long-lasting, slowly decaying depolarization lasting for several hundred ms. We also examine the receptor subtype involved. At least 3 distinct brain nicotinic acetylcholine receptors can be distinguished using pharmacological means. This include the MLA and bungarotoxin sensitive Type 1 receptors that are primarily composed of α7 subunits, the β2 subunit containing Type 2 receptors which can be identified by low micromolar block with DHβE and finally a less well characterized MLA and DHβE insensitive class of receptors (Type 3 receptors) that are blocked by low micromolar MEC (Alkondon and Albuquerque, 1993). The depolarization was resistant to the Type 1 nicotinic receptor antagonist, MLA (500 nM), and the Type 2 nicotinic receptor antagonist, DHβE (1 μM). However, all responses to carbachol were completely abolished by the weakly subtype-selective nicotinic receptor antagonist mecamylamine (MEC) applied at a concentration (5 μM) at which Type 1 and 2 receptors are not affected Fig. 5A1. In contrast, Type II THINs, responded to similar carbachol application with small-amplitude, brief depolarizations that rarely elicited action potentials and never triggered PPs (Fig. 5A2). Finally, Type IV THINs, the second most abundant THIN subtype comprising approximately 25% of striatal THINs, also responded to carbachol with a robust, long lasting depolarization that produced sustained firing, similar to the responses of Type I THINs. The pharmacological profile of Type IV THINs was the same as that of the Type I neurons.

Carbachol elicited similar, large amplitude, long-lasting membrane depolarization in the presence of TTX (1 μM) in Type I ($n = 4$) and Type IV ($n = 3$), THINs (Fig. 5B) that was completely blocked by MEC (5 μM). These data show that at least 2 types of THINs express nicotinic receptors. Interestingly, however, and similar to previous responses observed in striatal FSIs that also exhibit strong excitatory nicotinic responses to exogenous agonist application (Koós and Tepper, 2002), local electrical stimulation of the striatum failed to evoke any nicotinic synaptic response in THINs of any subtypes tested (data not shown).

4. Discussion

The present experiments examined the effects of DA and ACh on striatal THINs. The first principal finding was that intrinsic PPs elicited by depolarizing pulses in Type I and Type II THINs were facilitated by DA acting through a D1/D5-like DA receptor, and that in Type I and Type II THINs that did not exhibit intrinsic PPs, as well as in Type IV THINs that were never observed to exhibit intrinsic PPs, these plateaus could be elicited by D1/D5 receptor stimulation. In all cases, the PPs were primarily mediated by the non-selective cation conductance, I_{CAN}.

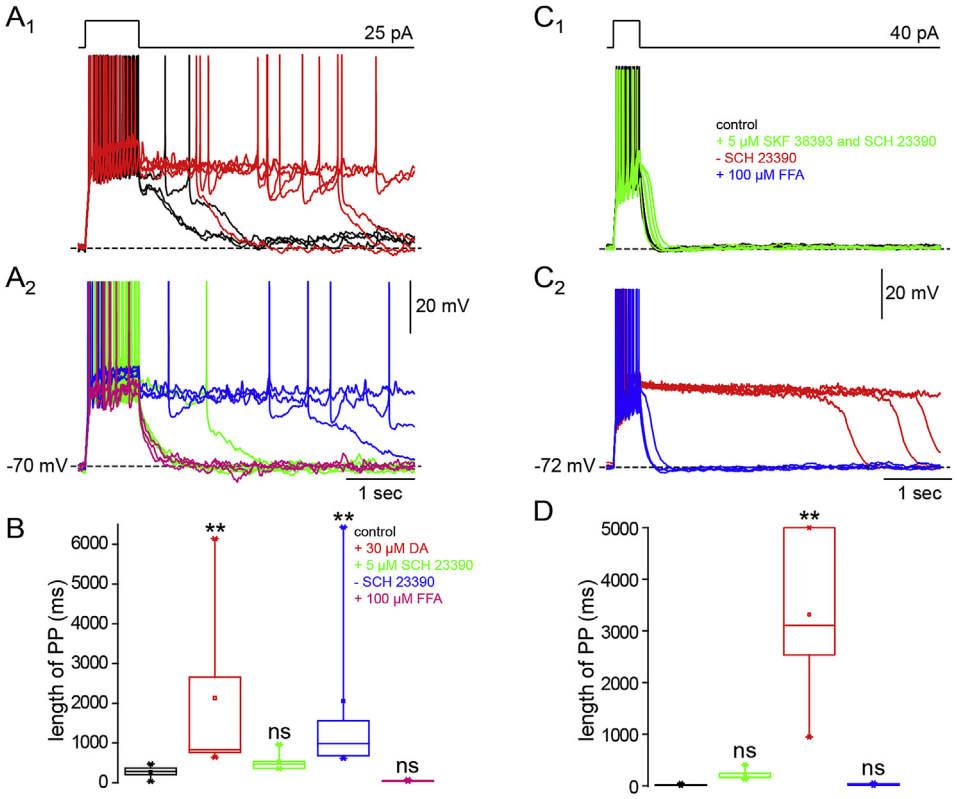

Fig. 4. Intrinsic PPs are facilitated by DA acting through D1/D5 DA receptors in striatal THINs. A1. Intrinsic PP in a Type I THIN (black traces) is greatly prolonged by addition of 30 μM DA (red traces). A2. Subsequent addition of SCH-23390 (5 μM), a selective D1/D5 DA receptor antagonist, first reduced and then completely blocked PPs (green traces). This effect washed out completely when the SCH-23390 was removed and the PP returned (blue traces). Either FFA (100 μM) or NIM (10 μM; not shown), completely blocked the PP. B. Summary box plots of six experiments on effects of DA and SCH 23390. See Fig. 2 legend for explanation. C1. Striatal Type IV THIN does not exhibit PP (black traces) under control condition. Simultaneous addition of both SCH-23390 (5 μM) and 5 μM SKF-38393 does not affect the PP (green traces). C2. Subsequent removal of SCH23390 instates the PP. The PP is completely blocked by addition of 100 μM FFA. Summary box plots of five experiments. Action potentials are truncated to illustrate subthreshold events. (For interpretation of the references to color in this figure legend, the reader is referred to the web version of this article.)

Finally, all subtypes of striatal THINs tested responded to brief pressure application of the non-selective cholinergic agonist, carbachol, with depolarization and excitation, whose strength greatly varied by subtype. In all cases, the response was shown to be due to direct activation of a nicotinic receptor distinct from the DHβE sensitive and MLA sensitive receptors.

4.1. Plateau potentials in striatal THINS are mediated by I_{CAN}

The present results elaborate on our earlier findings regarding the ionic mechanism of PPs and identify some of the specific contributions of I_{CAN} and L-type channels to the initiation and maintenance of PPs. Deletion of sodium from the extracellular solution greatly reduced the duration of the PPs but did not completely block them while subsequent removal of calcium and/or blockade of L-type Ca^{2+} channels by nimodipine completely eliminated the remaining PP. The PP was insensitive to TTX. In addition, the PP was completely blocked by flufenamic acid an antagonist of a melastatin-related transient receptor potential cation channel isoform (TRPM2) that underlies a calcium activated nonselective cationic conductance, I_{CAN} (Fleig and Penner, 2004; Hill et al., 2004; Lee and Tepper, 2007; Lee et al., 2013). Moreover, as shown earlier (Ibáñez-Sandoval et al., 2011) blockade of L-Type channels prevents PPs in THINs in response to response to depolarization. Therefore, the most likely ionic mechanism of the initiation of the PP is Ca^{2+} entry through L-type channels in response to depolarization leading to activation of I_{CAN}. I_{CAN} activation may also involve Ca^{2+} induced Ca^{2} release (CICR) from intracellular stores initiated by Ca^{2+} entry through L-type channels and possibly aided by a non-conventional $G_{q/11}$-coupled IP_3 signaling pathway of D_1 DA receptors (Rashid et al., 2007).

Interestingly, although many Type I and Type II THINS expressed intrinsic THINS, in those cells that did not, PPs could be elicited in essentially all striatal THINs (including Type IV THINs, c.f. Fig. 2B) by blocking a TEA-sensitive potassium conductance, as reported for other I_{CAN} expressing neurons of the basal ganglia (Lee and Tepper, 2007).

It is less clear what mechanism accounts for the termination of the PPs. Slow inactivation of L-type channels is one possibility. Alternatively if activation of I_{CAN} relies on calcium induced calcium release from intracellular stores, store depletion or desensitization of IP3 receptors may be involved.

4.2. Plateau potentials in striatal THINS are modulated by dopamine

The duration of intrinsic PPs was greatly increased by bath application of DA or the selective D1/D5 DA receptor agonist, SKF38393. Further PPs could be elicited in striatal THINs that did not exhibit intrinsic PPs by application of exogenous DA or amphetamine-induced release of endogenous DA. These effects were abolished by concomitant or subsequent application of the selective D1/D5 DA receptor antagonist, SCH-23390. These effects are consistent with a recent study that showed that intrinsic PPs in striatal THINs were greatly reduced in duration or completely eliminated in striata of mice that had received complete

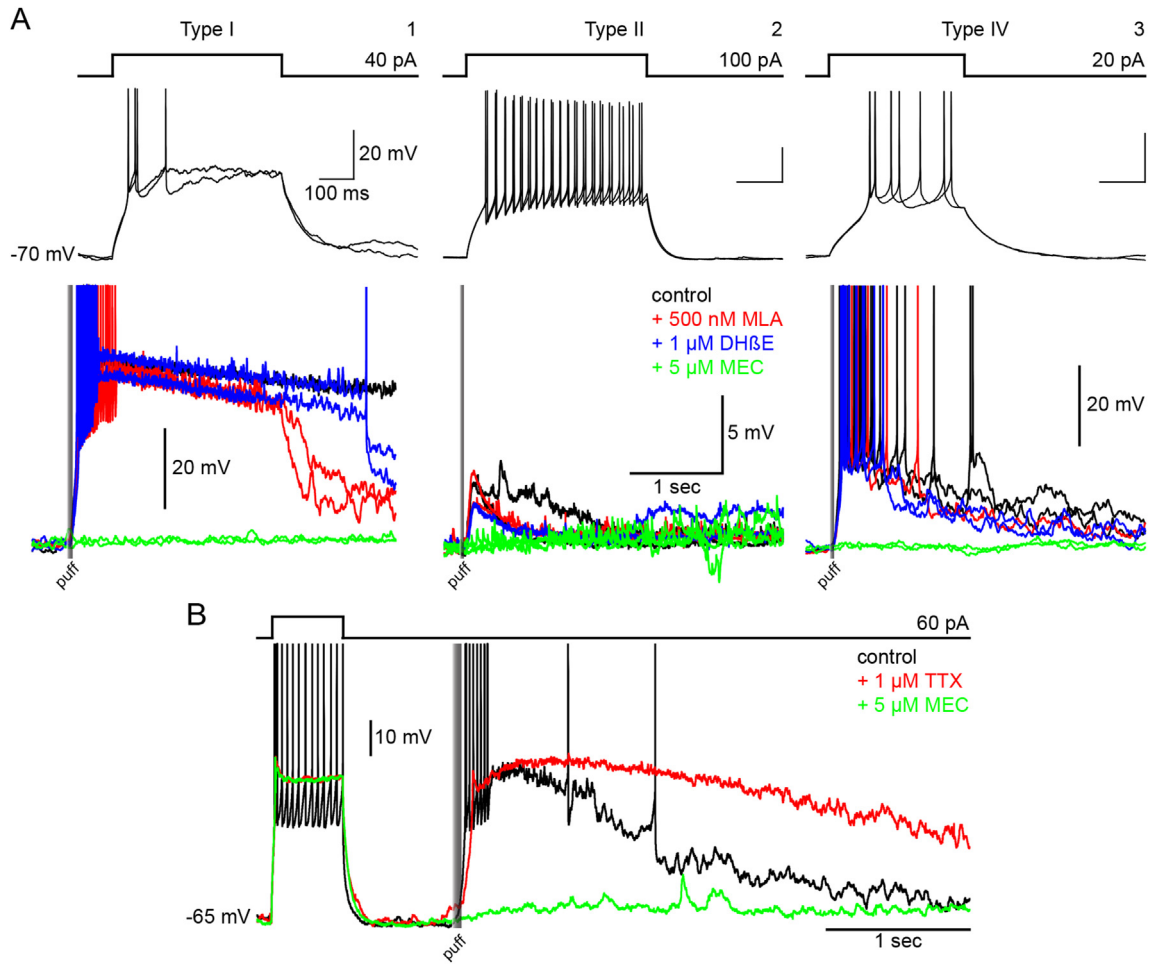

Fig. 5. Striatal THINs are excited by Type 3 nicotinic cholinergic receptors. A1-3. Type I, II and IV striatal THINs are depolarized by local pressure application of the non-selective cholinergic agonist, carbachol. The effects of carbachol vary in intensity with THIN subtype. Type I shows a strong depolarization accompanied the onset of action potentials, followed by a long duration depolarization with spikes completely blocked, consistent with the response of Type I THINs to current injection (1). In contrast, Type II THINs showed a small but consistent depolarization that was accompanied on some occasions by action potentials (not shown) (2). Type IV THINs also exhibited a strong depolarization with spikes throughout, consistent with the response of this Type IV THINs to current injection (3). For all cell types, carbachol-induced depolarization was unaffected by MLA (500 nM), an antagonist of Type 1 nicotinic receptors (red traces) or by DHßE (1 µM), a Type 2 nicotinic receptor antagonist (blue traces) but was totally blocked by blocked by MEC (5 µM), a Type 3 nicotinic receptor antagonist (green traces). Note different voltage calibrations for 1 and 3 vs. 2. B. The effect of carbachol persists even in presence of TTX (red trace), showing that it is a direct postsynaptic effect. In the present of TTX, MEC (5 µM) still completely blocked the effects of carbachol (green trace). Action potentials are truncated to illustrate subthreshold events. (For interpretation of the references to color in this figure legend, the reader is referred to the web version of this article.)

denervation of the nigrostriatal dopaminergic pathway one week earlier (Unal et al., 2015).

Like intrinsic PPs, dopamine-induced or facilitated PPs were completely abolished by nimodipine suggesting that dopamine promotes Ca^{2+} influx through L-type calcium channels or by flufenamic acid, that also blocks a non-selective cation conductance activated by calcium influx through L-type Ca^{2+} channels (Fleig and Penner, 2004; Hill et al., 2004; Lee and Tepper, 2007; Lee et al., 2013).

We did not attempt to identify the exact ionic mechanism of the dopaminergic enhancement of PPs. DA is well known to enhance L-type currents through D1/D5 receptors in a number of different neurons including SPNs (Surmeier et al., 1995; Hernández-López et al., 1997). Since the DA induced or modulated PPs in THINS were L-type channel dependent a similar mechanism may underly the effect of DA. Previous studies utilizing D1 knockout mice showed that the excitatory effects of dopamine and D1/D5 DA agonists on both striatal FSIs (Bracci et al., 2002) and PLTS (Centonze et al., 2002) interneurons persist in the D1 knockout mice suggesting that they are in fact mediated by the D5 receptor (Centonze et al., 2003). Both receptor subtypes have been shown to be expressed by various striatal neurons, with the D1 receptor being present in much greater abundance, especially by SPNs. Interneurons, on the other hand, including PV + FSIs, somatostatin-expressing PLTS neurons as well as cholinergic interneurons express relatively high levels of the D5 receptor while CR interneurons express low to moderate levels (Rivera et al., 2002). Perhaps D5 receptor expression is a general property shared by all striatal interneurons and that these receptors are also responsible for the dopaminergic facilitation of PPs in striatal THINs.

It is important to note that the effect of dopamine on PPs is the most dramatic direct effect on the excitability of any striatal neurons described to date. Of particular interest, this effect was readily elicited by endogenously released dopamine and therefore its magnitude is probably well within what can be expected to occur under physiological elevations of extracellular dopamine concentration *in vivo*.

4.3. Striatal TH interneurons express Type 3 nicotinic ACh receptors

Striatal ACh interacts with both metabotropic muscarinic and ionotropic nicotinic receptors at a variety of cellular and subcellular locations. Muscarinic receptors are widely expressed

postsynaptically on striatal SPNs and interneurons where they modulate excitability in a complex state- and cell-type specific but generally facilitatory way (Figueroa et al., 2002; Perez-Rosello et al., 2005; Shen et al., 2005, 2007) Muscarinic receptors are also present on GABAergic (Koós and Tepper, 2002) and glutamatergic terminals (Pakhotin and Bracci, 2007) where they generally exhibit powerful presynaptic inhibitory effects (Zhou et al., 2003). Nicotinic receptors, in contrast, are largely restricted to striatal interneurons (Goldberg et al., 2012) where they exert excitatory effects on GABAergic interneuron firing (English et al., 2012; Koós and Tepper, 2002), and are also present on DA terminals (Marshall et al., 2002) where it has been proposed that they may elicit DA release independent of DA neuronal activity (Cachope et al., 2012; Threlfell et al., 2012).

Striatal THINs exhibit a depolarization in response to locally applied carbachol that was unaffected by MLA or DHβE, but abolished by mecamylamine, a selective Type 3 nicotinic receptor agonist. This nicotinic receptor profile differs from that striatal FSIs and NPY-NGF GABAergic interneurons (Koós and Tepper, 2002; English et al., 2012) but is consistent with a recent report by Luo et al. (2013) that found the same antagonist sensitivities for striatal Type I THINs as we report here, and additionally demonstrated that striatal Type I THINs respond to cytisine, a selective α3β4 agonist nicotinic agonist. Here we show additionally that although all THINs tested exhibited a nicotinic excitation with a similar or identical pharmacology, there appeared to be subtype-specific differences in the strength of the excitation. The reasons for these differences remain unclear.

4.4. Physiological relevance

The nonspecific cationic conductance, I_{CAN}, is ubiquitously expressed in neurons from a number of different basal ganglia nuclei, including nigrostriatal dopaminergic neurons (Ping and Shepard, 1999; Yamashita and Isa, 2003, 2004), GABAergic substantia nigra pars reticulata projection (Lee and Tepper, 2007; Lee et al., 2013), glutamatergic subthalamic nucleus neurons (Baufreton et al., 2003), as well as striatal SPNs (Bao et al., 2005; Vergara et al., 2003) and THINs, and likely causes a generalized increase in the excitability of these neurons, amplifying excitatory afferents and affecting their firing pattern (Yamashita and Isa, 2003; Lee and Tepper, 2007). DA activates THINS directly through a D1/D5 receptor, which in turn leads to powerful feed-forward inhibition of SPNs (Ibáñez-Sandoval et al., 2010). THINs are also subject to fast nicotinic excitation by ACh released from striatal cholinergic interneurons, as are NPY-NGF interneurons, which also provide feed-forward inhibition of SPNs (Ibáñez-Sandoval et al., 2011; English et al., 2012).

During the learning process in primates a cue associated with reward or other salient event evokes a pause in the tonic activity of cholinergic interneurons (CIN) in the striatum sometimes preceded by an increase in firing and often followed by a rebound excitation (Aosaki et al., 1994, 1995, 2010), while the same stimulus triggers an increase in the firing rate of midbrain dopaminergic neurons and striatal DA release concomitant with the pause part of the CIN sequence. While the pause may not affect the ongoing firing rate of striatal SPNs (English et al., 2012; but the situation may be different in the ventral striatum; see Witten et al., 2010), the rebound causes a powerful feed-forward disynaptic inhibition of SPNs. The SPN inhibition is caused by Type 2 nicotinic receptor mediated cholinergic activation of NPY-NGF GABAergic interneurons that produce a $GABA_A$ IPSC in the SPN that exhibits unusually slow kinetics (Ibáñez-Sandoval et al., 2011). The rebound also activates a recurrent IPSC in the CIN mediated through a different, as yet unidentified, GABAergic interneuron that is also activated by Type 2 nicotinic receptors but that displays typical fast $GABA_A$ kinetics (Sullivan et al., 2008; English et al., 2012).

Thus, the arrival of a salient, reward predicting stimulus will first trigger a dopaminergic response that will increase the excitability of striatal THINs, followed a few hundred ms later by a slower onset of prolonged activation of both THINs and NPY-NGF interneurons as the CINs rebound from the pause. The CIN rebound may also elicit a prolonged secondary release of DA by acting directly at nigrostriatal terminals (Cachope et al., 2012; Threlfell et al., 2012).

Consequently, the activation of feed-forward inhibition of SPNs following dopaminergic and cholinergic activation involves at least two different populations of GABAergic interneurons that are activated sequentially and whose inhibition of SPNs exhibits different time courses and kinetics. The precise roles that these two forms of feed-forward inhibition play in the signaling of salience and reward in striatum are not yet known, but for striatal THINs alone, the initial facilitation of their excitability by the nigrostriatal dopaminergic reward prediction error signal followed by the subsequent activation by the CIN rebound suggests that they play a role distinct from that of FSIs and NPY-NGF interneurons during the acquisition of associative learning in striatum.

Acknowledgments

This research was supported, in part, by NIH Grants 5R01NS034865 (J M T.), 1R01NS072950 (T K. and J.M. T.) and Rutgers University. We thank Fulva Shah and Parth Gandhi for excellent technical assistance and Leticia Maldonado for the biocytin reconstruction in Figure 1A.

References

Adams, J.C., 1981. Heavy metal intensification of DAB-based HRP reaction product. J. Histochem. Cytochem. 29 (6), 775.
Alkondon, M., Albuquerque, E.X., 1993. Diversity of nicotinic acetylcholine receptors in rat hippocampal neurons. I. Pharmacological and functional evidence for distinct structural subtypes. J. Pharmacol. Exp. Ther. 265, 1455–1473.
Aosaki, T., Graybiel, A.M., Kimura, M., 1994. Effect of the nigrostriatal dopamine system on acquired neural responses in the striatum of behaving monkeys. Science 265, 412–415.
Aosaki, T., Kimura, M., Graybiel, A.M., 1995. Temporal and spatial characteristics of tonically active neurons of the primate's striatum. J. Neurophysiol. 73, 1234–1252.
Aosaki, T., Miura, M., Suzuki, T., Nishimura, K., Masuda, M., 2010. Acetylcholine–dopamine balance hypothesis in the striatum: an update. Geriatr. Gerontol. Int. 10 (suppl. 1), S148–S157.
Bao, L., Avshalumov, M.V., Rice, M.E., 2005. Partial mitochondrial inhibition causes striatal dopamine release suppression and medium spiny neuron depolarization via H_2O_2 elevation, not ATP depletion. J. Neurosci. 25, 10029–10040.
Baufreton, J., Garret, M., Rivera, A., de la Calle, A., Gonon, F., Dufy, B., Bioulac, B., Taupignon, A., 2003. D5 (not D1) dopamine receptors potentiate burst- firing in neurons of the subthalamic nucleus by modulating an L-type calcium conductance. J. Neurosci. 23, 816–825.
Bracci, E., Centonze, D., Bernardi, G., Calabresi, P., 2002. Dopamine excites fast-spiking interneurons in the striatum. J. Neurophysiol. 87, 2190–2194.
Cachope, R., Mateo, Y., Mathur, B.N., Irving, J., Wang, H.L., Morales, M., Lovinger, D.M., Cheer, J.F., 2012. Selective activation of cholinergic interneurons enhances accumbal phasic dopamine release: setting the tone for reward processing. Cell. Rep. 2, 33–41.
Centonze, D., Bracci, E., Pisani, A., Gubellini, P., Bernardi, G., Calabresi, P., 2002. Activation of dopamine D_1-like receptors excites LTS interneurons of the striatum. Eur. J. Neurosci. 15, 2049–2052.
Centonze, D., Grande, C., Usiello, A., Gubellini, P., Erbs, E., Martín, A.B., Pisani, A., Tognazzi, N., Bernardi, G., Moratalla, R., Borrelli, E., Calabresi, P., 2003. Receptor subtypes involved in the presynaptic and postsynaptic actions of dopamine in striatal interneurons. J. Neurosci. 23, 6245–6254.
DeFelipe, J., López-Cruz, P.L., Benavides-Piccione, R., Bielza, C., Larrañaga, P., et al., 2013. New insights into the classification and nomenclature of cortical GABAergic interneurons. Nat. Rev. Neurosci. 14, 202–216.
English, D.F., Ibáñez-Sandoval, O., Stark, E., Tecuapetla, F., Buzsáki, G., Deisseroth, K., Tepper, J.M., Koós, T., 2012. GABAergic circuits mediate the reinforcement-related signals of striatal cholinergic interneurons. Nat. Neurosci. 15, 123–130.
Figueroa, A., Galarraga, E., Bargas, J., 2002. Muscarinic receptor involved in the subthreshold cholinergic actions of neostriatal spiny neurons. Synapse 46, 215–223.

Fleig, A., Penner, R., 2004. The TRPM ion channel subfamily: molecular, biophysical and functional features. Trends Pharmacol. Sci. 25, 633–639.
Freund, T.F., Buzsáki, G., 1996. Interneurons of the hippocampus. Hippocampus 6 (4), 347–470.
Goldberg, J.A., Ding, J.B., Surmeier, D.J., 2012. Muscarinic modulation of striatal function and circuitry. Handb. Exp. Pharmacol. 208, 223–241.
Gong, S., Zheng, C., Doughty, M.L., Losos, K., Didkovsky, N., Schambra, U.B., Nowak, N.J., Joyner, A., Leblanc, G., Hatten, M.E., Heintz, N., 2003. A gene expression atlas of the central nervous system based on bacterial artificial chromosomes. Nature 425, 917–925.
Hernández-López, S., Bargas, J., Surmeier, D.J., Reyes, A., Galarraga, E., 1997. D_1 receptor activation enhances evoked discharge in neostriatal medium spiny neurons by modulating an L-type Ca^{2+} conductance. J. Neurosci. 17, 3334–3342.
Hill, K., Benham, C.D., McNulty, S., Randall, A.D., 2004. Flufenamic acid is a pH-dependent antagonist of TRPM2 channels. Neuropharmacology 47, 450–460.
Ibáñez-Sandoval, O., Tecuapetla, F., Unal, B., Shah, F., Koós, T., Tepper, J.M., 2010. Electrophysiological and morphological characteristics and synaptic connectivity of tyrosine hydroxylase-expressing neurons in adult mouse striatum. J. Neurosci. 30, 6999–7016.
Ibáñez-Sandoval, O., Tecuapetla, F., Unal, B., Shah, F., Koós, T., Tepper, J.M., 2011. A novel functionally distinct subtype of striatal neuropeptide Y interneuron. J. Neurosci. 31, 16757–16769.
Kahlig, K.M., Binda, F., Khoshbouei, H., Blakely, R.D., McMahon, D.G., Javitch, J.A., Galli, A., 2005. Amphetamine induces dopamine efflux through a dopamine transporter channel. Proc. Natl. Acad. Sci. U. S. A. 102, 3495–3500.
Khoshbouei, H., Wang, H., Lechleiter, J.D., Javitch, J.A., Galli, A., 2003. Amphetamine-induced dopamine efflux. A voltage-sensitive and intracellular Na+-dependent mechanism. J. Biol. Chem. 278, 12070–12077.
Koós, T., Tepper, J.M., 2002. Dual cholinergic control of fast-spiking interneurons in the neostriatum. J. Neurosci. 22, 529–535.
Lee, C.R., Tepper, J.M., 2007. A calcium-activated nonselective cation conductance underlies the plateau potential in rat substantia nigra GABAergic neurons. J. Neurosci. 27, 6531–6541.
Lee, C.R., Machold, R.P., Witkovsky, P., Rice, M.E., 2013. TRPM2 channels are required for NMDA-induced burst firing and contribute to H_2O_2-dependent modulation in substantia nigra pars reticulata GABAergic neurons. J. Neurosci. 33, 1157–1168.
Luo, R., Janssen, M.J., Partridge, J.G., Vicini, S., 2013. Direct and GABA-mediate indirect effects of nicotinic ACh receptor agonists on striatal neurones. J. Physiol. 591, 203–217.
Marshall, D.L., Redfern, P.H., Wonnacott, S., 2002. Presynaptic nicotinic modulation of dopamine release in the three ascending pathways studied by in vivo microdialysis: comparison of naive and chronic nicotine-treated rats. J. Neurochem. 68, 1511–1519.
Pakhotin, P., Bracci, E., 2007. Cholinergci interneurons control the exhitatory input to the striatum. J. Neurosci. 27, 391–400.
Perez-Rosello, T., Figueroa, A., Salgado, H., Vilchis, C., Tecuapetla, F., Guzman, J.N., Galarraga, E., Bargas, J., 2005. Cholinergic control of firing pattern and neurotransmission in rat neostriatal projection neurons: role of $Ca_v2.1$ and $Ca_v2.2$ Ca^{2+} channels. J. Neurophysiol. 93, 2507–2519.
Ping, H.X., Shepard, P.D., 1999. Blockade of SK-type Ca^{2+}-activated K channels uncovers a Ca^{2+}-dependent slow afterdepolarization in nigral dopamine neurons. J. Neurophysiol. 81, 977–984.
Rashid, A.J., So, C.H., Kong, M.M.C., Furtak, T., El-Ghundi, M., Cheng, R., O'Dowd, B.F., George, S.R., 2007. D1–D2 dopamine receptor heterooligomers with unique pharmacology are coupled to rapid activation of G_q/11 in the striatum. PNAS 104 (2), 654–659.
Rivera, A., Alberti, L., Martín, A.B., Narváez, J.A., de la Calle, A., Moratalla, R., 2002. Molecular phenotype of rat striatal neurons expressing the dopamine D5 receptor subtype. Eur. J. Neurosci. 16, 2049–2058.
Shen, W., Hamilton, S.E., Nathanson, N.M., Surmeier, D.J., 2005. Cholinergic suppression of KCNQ channel currents enhances excitability of striatal medium spiny neurons. J. Neurosci. 25, 7449–7458.
Shen, W., Tian, X., Day, M., Ulrich, S., Tkatch, T., Nathanson, N.M., Surmeier, D.J., 2007. Cholinergic modulation of Kir2 channels selectively elevates dendritic excitability in striatopallidal neurons. Nat. Neurosci. 10, 1458–1466.
Sullivan, M.A., Chen, H., Morikawa, H., 2008. Recurrent inhibitory network among striatal cholinergic interneurons. J. Neurosci. 28, 8682–8690.
Surmeier, D.J., Bargas, J., Hemmings Jr., H.C., Nairn, A.C., Greengard, P., 1995. Modulation of calcium currents by a D1 dopaminergic protein kinase/phosphatase cascade in rat neostriatal neurons. Neuron 14, 385–397.
Tepper, J.M., Tecuapetla, F., Koós, T., Ibáñez-Sandoval, O., 2010. Heterogeneity and diversity of striatal GABAergic interneurons. Front. Neuroanat. 4, 150. http://dx.doi.org/10.3389/fnana.2010.00150.
Threlfell, S., Lalic, T., Platt, N.J., Jennings, K.A., Deisseroth, K., Cragg, S.J., 2012. Striatal dopamine release is triggered by synchronized activity in cholinergic interneurons. Neuron 75, 58–64.
Unal, B., Ibáñez-Sandoval, O., Shah, F., Abercrombie, E.D., Tepper, J.M., 2011. Distribution of tyrosine hydroxylase expressing interneurons with respect to anatomical organization of the neostriatum. Front. Syst. Neurosci. 5, 41. http://dx.doi.org/10.3389/fnsys.2011.00041.
Unal, B., Shah, F., Kothari, J., Tepper, J.M., 2015 Jan. Anatomical and electrophysiological changes in striatal TH interneurons after loss of the nigrostriatal dopaminergic pathway. Brain Struct. Funct. 220 (1), 331–349. http://dx.doi.org/10.1007/s00429-013-0658-8. Epub 2013, Oct 31.
Vergara, R., Rick, C., Hernández-López, S., Laville, J.A., Guzman, J.N., Galarraga, E., Surmeier, D.J., Bargas, J., 2003. Spontaneous voltage oscillations in striatal projection neurons in a rat corticostriatal slice (Lond). J. Physiol. 553, 169–182.
Witten, I.B., Lin, S.C., Brodsky, M., Prakash, R., Diester, I., Anikeeva, P., Gradinaru, V., Ramakrishnan, C., Deisseroth, K., 2010. Cholinergic interneurons control local circuit activity and cocaine conditioning. Science 330, 1677–1681.
Yamashita, T., Isa, T., 2003. Fulfenamic acid sensitive, Ca^{2+}-dependent in- ward current induced by nicotinic acetylcholine receptors in dopamine neurons. Neurosci. Res. 46, 463–473.
Yamashita, T., Isa, T., 2004. Enhancement of excitatory postsynaptic poten- tials by preceding application of acetylcholine in mesencephalic dopamine neurons. Neurosci. Res. 49, 91–100.
Zhou, F.M., Wilson, C.J., Dani, J.A., 2003. Muscarinic and nicotinic cholinergic mechanisms in the mesostriatal dopamine systems. Neuroscientist 9, 23–36.